Journal of Radioanalytical and Nuclear Chemistry (2025) 334:7009–7018
https://doi.org/10.1007/s10967-025-10347-0

Development and validation of the k_0-standardization based neutron activation analysis (k_0-NAA) at NUR research reactor

A. Guesmia[1,2] · L. Hamidatou[3] · H. Slamene[4] · T. Azli[3] · M. E. A. Benamar[5]

Received: 20 January 2025 / Accepted: 11 August 2025 / Published online: 26 September 2025

Abstract
This study evaluates the k_0-INAA method at Algeria's NUR reactor for precise multi-element analysis. The HPGe detector was calibrated for accurate gamma-ray spectrometry, while reactor calibration characterized neutron fluxes and alpha and *f* spectrum parameters using triple monitor method in three NAA channels covering short, medium and long irradiation. The k_0-standardization method was applied to geological (CRM-GSD12) and biological (SRM-NIST1573a) reference materials, with quality assurance through ratio analysis and Zeta-score evaluation. Results showed strong agreement with certified values, with most Zeta-scores within ± 1, confirming the method's precision and reliability for elemental analysis under optimized calibration and irradiation conditions.

Keywords k_0-INAA · NUR research reactor · Neutron flux parameters · Validation · Trace elements

Introduction

The NUR research reactor, located at the Nuclear Research Center of Draria (CRND) in Algiers, Algeria, is a pivotal facility in the country's nuclear research and development efforts. Commissioned in 1989, the NUR reactor is an open pool-type reactor with a nominal thermal power of 1 MW. It is primarily used for research, education, and training purposes, as well as for the production of radioisotopes on a laboratory scale, neutron activation analysis and neutron radiography. The reactor's design and operational capabilities make it an essential tool for advancing nuclear science and technology in Algeria [1–5].

✉ A. Guesmia
a-guesmia@crnd.dz

1 Reactor Division, Nuclear Research Center of Draria, Algiers, Algeria

2 Energy and Materials Laboratory, University of Tamanghasset, 11001 Tamanghasset, Algeria

3 Nuclear Research Centre of Draria, Algiers, Algeria

4 Nuclear Research Centre of Birine, PoBox 180, 17200 Ain Oussera, Djelfa, Algeria

5 Department of Science and Technology, University of Tamanghasset, 11001 Tamanghasset, Algeria

Since 1993, Instrumental neutron activation analysis (INAA) has been actively employed at the NUR research reactor using relative standardization method for analyzing geological, biological, and environmental samples [6–9]. While this method is known for its high accuracy and precision, it has certain limitations. This includes the necessity for standard materials, which can be time-consuming to prepare and counting, and the need for irradiation and counting under controlled conditions. Moreover, unexpected elements can complicate the analysis, particularly when multi-element analyses are required for large sample sets.

To address these challenges, the k_0-standardization method offers significant advantages. This approach makes the classical single-comparator "*k-factor*" technique more flexible regarding irradiation and counting conditions. It also enhances the accuracy of the absolute method by replacing individual nuclear data with compound nuclear data, denoted as k_0-factors, which are experimentally determined with high precision. Since its development in the mid-1970s by F. De Corte, A. Simonits, and collaborators [10], the k_0-based neutron activation analysis method has been widely adopted by research reactors worldwide [11–17]. In its current ready-to-use form, it is recognized as an efficient, practical, and reliable NAA standardization technique [18].

In Algeria, the k_0-NAA method was first introduced successfully at the Es-Salam research reactor in 2004 by L. Hamidatou et al., where the HØGDAHL convention and

WESTCOTT formalism were applied [12, 19, 20]. This technique is extensively used in various fields, such as geology, biology, materials science, and environmental studies [21–24], providing a complementary tool to other sensitive and accurate non-nuclear analytical techniques.

The main objective of this study is to implement and validate the k_0-INAA procedure at the NUR research reactor. This involves determining the detection efficiency of the HP Ge detector and estimating neutron flux parameters at the selected irradiation facilities using the triple-bare flux monitors method. The procedure is evaluated by applying it to geological and biological standard reference materials.

Implementation methodology

The k_0-NAA method for element concentration determination is based on the Høgdahl formalism. According to this approach, the concentration of an element in *mg/kg*, ρ can be calculated using the following equation [10, 16, 25]:

$$\rho = \frac{\left(\frac{N_p}{t_m SDCW}\right)_a}{\left(\frac{N_p}{t_m SDCw}\right)_c} \frac{1}{k_0} \frac{f + Q_{0,c}(\alpha)}{f + Q_{0,a}(\alpha)} \frac{\varepsilon_{p,c}}{\varepsilon_{p,a}} \quad (1)$$

where the subscripts a and c refer to the analyte and the comparator, respectively, N_p is the net peak area, t_m is the measurement time, S, D, and C are the saturation factor, decay correction factor, and counting correction factor, respectively, W is the sample weight (in g) and w is the comparator weight (in µg), ε_p is the full-energy peak efficiency, f is the thermal-to-epithermal neutron flux ratio, Q_0 is the resonance integral-to-thermal cross-section ratio (I_0/σ_0), α is the epithermal non-ideality factor, which expresses deviation from the ideal $1/E$ neutron energy distribution. The actual neutron flux distribution, denoted as $1/E^{1+\alpha}$, is used to correct the resonance integral.

The k_0-factors are nuclear constants that replace absolute nuclear data. These constants have been experimentally determined, and distributed by IUPAC freely on request, and those nuclear data were updated several times by the k_0-ISC (https://www.kayzero.com) during the last 20 years in the Excel file.

From Eq. (1), we see that while k_0-factors are reactor and detector independent, the implementation of k_0-NAA still requires experimental determination of both the ε_p and the neutron flux parameters (f and α), which are specific to the measurement facility and irradiation position, respectively. Various experimental methods are used for determining the parameters f and α. Some methods require the use of a cadmium cover, such as the Cd-covered multi-monitor method and the Cd-ratio for multi-monitor technique. Others, like the bare multi-monitor method, do not require a Cd-cover and allow for instantaneous determination of f and α [12, 25–27].

In particular, the bare triple-monitor method uses three monitors, with the most common set being ^{94}Zr, ^{96}Zr, and ^{197}Au, which allows the simultaneous determination of f and α [28]. In this work, this method was employed, and the values of f and α were calculated using well-established equations available in numerous references, [12, 16, 25].

The fast flux was determined based on the threshold reaction using Fe monitor for long irradiation channels and Al-Au monitor for short irradiation channel. The reactions used to calculate f, α and the fast flux $\emptyset_f$ as well as the nuclear data of the flux monitors are summarized in Table 1.

Experimental setup

Irradiation facility description

Regarding the NUR, the reactor core consists of MTR-LEU fuel type, 12 standard fuel assemblies, 5 control fuel assemblies are mounted at the top of the reactor pool and swing downward through the core between adjacent guide plates of control fuel elements, and surrounded by 15 graphite reflector blocks providing flexible configurations. A thermal column allows for different irradiation tests [4, 5].

For samples irradiation purposes, the NUR reactor is equipped with several vertical irradiation channels, two irradiation boxes positioned within the reactor core, as well as a dedicated hole in the thermal column suitable for long irradiation. Loading of samples into these irradiation boxes is conducted manually using a samples holder designed to accommodate aluminum capsules arranged in two vertical lines with inclined orientations.

Table 1 Key nuclear data for monitors used in neutron flux characterization (2020)

#	Reaction	E_r, eV	Q_0	Half-life	E_γ, keV	$k_{0,\,Au}$
1	^{96}Zr (n, γ) ^{97}Zr	338	251.6	16.9 h	743.3	1.24 E-05
2	^{94}Zr (n, γ) ^{95}Zr	6260	5.31	64.02 d	724.2	8.9 E-05
3	^{197}Au (n, γ) ^{198}Au	5.65	15.7	2.695 d	756.7	1.1 E-04
4	^{54}Fe (n, p) ^{54}Mn	–	–	312.29 d	411.8	1
5	^{27}Al (n, p) ^{27}Mg	–	–	9.46 min	834.8	–
					843.76	–

For INAA of short-lived nuclides, the NUR reactor is equipped with two fast Pneumatic Transfer Systems (PTS). These systems are linked to two specific locations: one within the reactor core (R1) and the other in the thermal column (R2) via tubes and an air supply line. At these transfer stations, samples are enclosed within polyethylene capsules, known as rabbits, and introduced into the loading/receiving station with each achieving transfer times of approximately 2 s. The irradiation duration is pre-set in the PTS controller unit, and the end-of-irradiation time is recorded automatically. Figure 1 illustrates the NUR reactor's core configuration (X-1), thermal column and the various irradiation positions available.

In the present study, two irradiation positions in the central box (IB1#A2 and IB1#B3), where the neutron flux is high and consists of three components (thermal, epithermal, and fast), were analyzed. Additionally, the well-thermalized position (PTS#R2) in the thermal column was also examined.

Detector calibration

The characterization of the detector, which includes energy calibration and the determination of detection efficiency, is a crucial step in the k_0-NAA method. In this study, gamma-ray measurements were conducted using a coaxial n-type HP Ge detector (model GR3019) manufactured by Canberra coupled to associated electronics, with a relative efficiency of 30% and an energy resolution of 2.0 keV at 1332.5 keV. The detector was shielded with 10 cm of low-background lead, and the measurement system was operated using Gamma Vision-32 software.

Experimental efficiencies were determined through the measurement of point radionuclide sources, including ^{241}Am, ^{133}Ba, ^{60}Co, ^{137}Cs, ^{152}Eu, and ^{22}Na (supplied by PTB), and ^{57}Co (supplied by LEA), covering an energy range from 59 to 1408 keV. Efficiency calibrations were performed.

using four counting geometries (G0, G2, G4, and G6), corresponding to distances of 1.2 cm, 5.5 cm, 9.5 cm, and 13.5 cm from the detector end-cap, respectively, as employed in routine measurements. The mono-energy sources were used to determine the peak-to-total ratio for the specified geometries, while all sources (mono and multi-energy) were utilized to establish the full-energy peak detection efficiency for the same geometries.

Preparation, irradiation and measurement

To determine the thermal, epithermal, and fast neutron fluxes, as well as the α and f factors, several flux monitors were used, including Au 0.1%-Al, Zr, and Fe. These monitors, in the form of metallic or alloyed foils and wires, were prepared as follows:

- Au 0.1%-Al: IRMM-530R A foil, 0.1 mm thick, 8 mm diameter (6 mm for short irradiation);
- Zr (99.5%): Alfa Aesar foil, 0.127 mm thick, 8 mm diameter (6 mm for short irradiation);
- Fe (99.98%): Reactor Experiments R/X wire, 0.2286 mm diameter, 4 mm length.

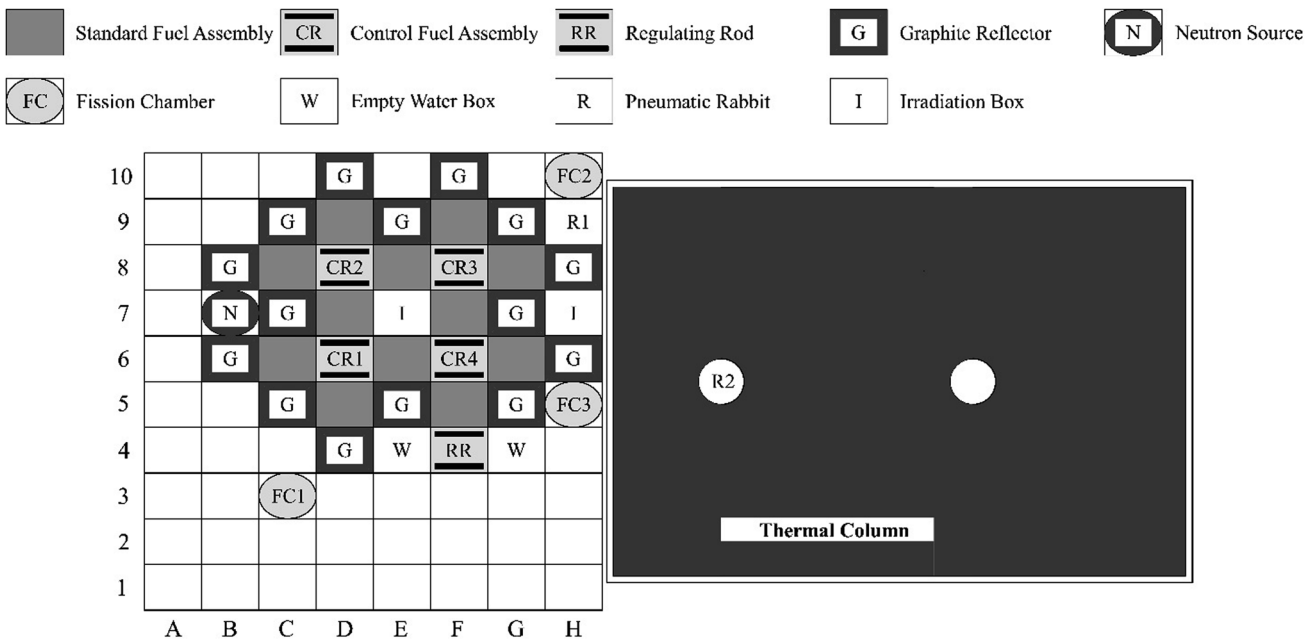

Fig. 1 NUR reactor's core configuration (X-1), thermal column and the various irradiation positions available

To evaluate the applicability and verify the procedure of the k_0-NAA method in our laboratory, two types of standards were used, triplicate samples of NIST 1573a (Biological Standard Reference Material) and GSD12 (Geological Certified Reference Material), samples weighing approximately 80 and 150 mg, respectively. These samples were packed in high-purity aluminum and wrapped with flux monitors, which were placed in each sample row to monitor the flux gradient inside the aluminum waterproof capsule. All samples were irradiated for 4 h.

Validation of the method at the short irradiation facility was carried out by irradiating the same standard materials. Approximately 80 mg of each sample was prepared in polyethylene vials (8 mm diameter, 20 mm height). Samples and flux monitors in similar vials were placed together in polyethylene rabbits and irradiated in PTS#R2 for a period of 60 to100 seconds depending on the sample matrix.

Regarding blank subtraction, the polyethylene (PE) vials used for sample irradiation contain trace impurities that can influence the measured concentrations of certain elements. To mitigate this effect, empty vials are irradiated and measured separately.

After irradiation and an appropriate decay period for each type of sample and monitor, measurements were performed using a calibrated HP Ge detector. All monitor measurements were performed at the reference distance (G6), the same distance used for samples during the first measurement. The second measurement was conducted at G2 to ensure good counting statistics.

Calculation

All gamma-ray spectra were analyzed using HyperLab 2023 [29]. Efficiency calibration of the high-purity germanium (HPGe) detector was performed using the Solcoi subroutine within the Kayzero/Solcoi software package [30, 31]. This routine applies coincidence summing corrections and geometrical efficiency adjustments based on the GR3019 detector specifications provided by the manufacturer, along with the experimentally determined dead layer thickness [32].

Neutron spectrum characterization was conducted using the bare triple monitor method, implemented in the Kayzero for Windows software (version 4). Elemental concentrations and their associated uncertainties were calculated within the software. To ensure accurate quantification, the options for correcting interferences from fast neutron-induced reactions [33], such as (n,p) and (n,α), as well as thermal neutron-induced uranium fission (when uranium is present in the samples), were explicitly enabled. Additionally, corrections for blank contributions from the irradiation vials were also selected.

Results and discussion

Efficiency calibration of HPGe

The Fig. 2 shows the efficiency curve of the GR3019 detector at the reference distance G6 (in a log–log plot), corresponding to the detector's response across photon energies (59–1500 keV). A polynomial fit models the efficiency for low-to-moderate energies (59–223 keV), reflecting higher sensitivity due to the photoelectric effect.

Beyond 223 keV, continually and with the same slope, a linear fit describes the decreasing efficiency as higher-energy photons interact less frequently. The transition at 223 keV marks a shift in interaction mechanisms, with Compton scattering becoming dominant. These findings ensure accurate efficiency corrections for precise quantitative gamma spectrometry in applications like neutron activation analysis.

Neutron flux characterization

The results in Table 2 provide key insights into the neutron spectrum parameters in the characterized irradiation facilities used for k_0-NAA. The thermal neutron flux Φ_{th} is highest in IB1#A2 $(2.40 \pm 0.02)10^{13}$ cm^{-2} s^{-1}, followed by IB1#B3 $(2.20 \pm 0.02)10^{13}$ cm^{-2} s^{-1} and then PTS#R2 $(2.29 \pm 0.04)10^{12}$ cm^{-2} s^{-1}, which has a significantly lower value. This indicates that IB1#A2 offers the most intense thermal neutron environment, ideal for isotopes relying on thermal neutron capture reactions, while PTS#R2 may serve specialized applications requiring lower thermal flux. Similarly, the fast neutron flux Φ_f is highest in IB1#A2 and lowest in PTS#R2, highlighting the diversity in neutron flux characteristics across facilities. The

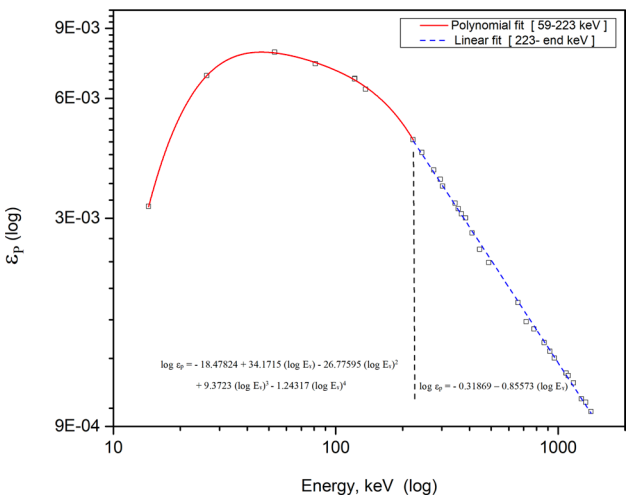

Fig. 2 The efficiency curve of the GR3019 detector at the reference distance 13.5 cm

Table 2 Neutron spectrum parameters in characterized irradiation facility for k_0-NAA

Irradiation facility	$Ø_{th}$ ($cm^{-2}. s^{-1}$)	$Ø_f$ ($cm^{-2}. s^{-1}$)	Neutron flux parameters	
			f	α
IB1#A2	$(2.40 \pm 0.02)\ 10^{13}$	$(9.89 \pm 0.08)\ 10^{12}$	21.56	−0.0343
IB1#B3			20.19	−0.0579
PTS#R2	$(2.20 \pm 0.02)\ 10^{13}$	$(9.19 \pm 0.08)\ 10^{12}$	61.24	−0.0226
	$(2.29 \pm 0.04)\ 10^{12}$	$(7.89 \pm 0.05)\ 10^{10}$		

neutron flux ratio f, representing the thermal to epithermal neutron flux ratio, is comparable in IB1#A2 and IB1#B3 (21.56 and 20.19, respectively), suggesting a balance between thermal and epithermal neutrons suitable for general-purpose k_0-NAA. On the other hand, PTS#R2 exhibits a much higher ratio (61.24), indicating a spectrum heavily dominated by thermal neutrons, making it ideal for applications requiring minimal epithermal interactions.

The epithermal neutron flux shape factor α, reflecting deviations in the epithermal neutron spectrum from an ideal 1/E distribution, is slightly negative in all facilities. PTS#R2 has the smallest deviation (−0.0226), suggesting a nearly ideal epithermal neutron spectrum, beneficial for accurately determining isotopes with significant resonance integrals.

In summary, IB1#A2 and IB1#B3 are versatile facilities offering high thermal neutron flux and balanced spectrum characteristics, suitable for general k_0-NAA applications. In contrast, PTS#R2 provides a specialized environment with a thermal neutron-dominant spectrum and an ideal epithermal neutron flux, making it optimal for precision applications. These results underline the importance of selecting an appropriate irradiation facility based on specific analytical objectives (Table 3).

Table 3 Analytical results of the CRM GSD12 (unit: mg/kg)

Element	Certified ± Unc (k = 2)	This work ± Unc (k = 2) at		
		IBI-A2	IBI-B3	PTS-R2
Ag	1.15 ± 0.11	1.15 ± 0.38	1.14 ± 0.23	49,000 ± 1500
Al	49,220 ± 582	–	–	–
As	115 ± 6	115.2 ± 3.9	115.2 ± 4.8	–
Ba	206 ± 15	230 ± 36	209 ± 44	–
Br	1.7 ± 0.4	1.6 ± 0.24	0.98 ± 0.12	–
Ce	61 ± 4	67.2 ± 1.4	60.7 ± 1.2	173 ± 34
Cl	163 ± 25	–	–	–
Co	8.8 ± 0.7	8.0 ± 0.6	7.4 ± 0.6	–
Cr	35 ± 3	44.4 ± 3.3	42.1 ± 1.5	–
Cs	7.9 ± 0.4	7.89 ± 0.09	7.91 ± 0.22	1240 ± 210
Cu	1230 ± 33	–	–	–
Eu	0.61 ± 0.03	0.63 ± 0.04	0.62 ± 0.02	–
Fe	34,132 ± 629	34,300 ± 490	35,000 ± 700	–
Hf	8.3 ± 1.0	8.28 ± 0.24	8.4 ± 0.6	1.05 ± 0.24
In	0.96 ± 0.15	–	–	24,300 ± 3000
K	24,157 ± 332	24,100 ± 240	24,160 ± 2561	–
La	32.7 ± 1.4	32.7 ± 1.5	31.1 ± 1.9	–
Lu	0.58 ± 0.06	0.73 ± 0.04	0.76 ± 0.06	17,630 ± 654
Mg	17,548 ± 241	–	–	1410 ± 140
Mn	1400 ± 47	–	–	3230 ± 220
Na	3264 ± 148	3220 ± 60	3190 ± 47	–
Nd	26 ± 3	30 ± 5	25.4 ± 3.9	–
Rb	270 ± 10	270 ± 10	258 ± 6	–
Sb	24 ± 3	24.31 ± 0.34	24.77 ± 0.38	–
Sc	5.1 ± 0.4	5.11 ± 0.27	4.89 ± 0.03	–
Sm	5.0 ± 0.4	5.5 ± 0.6	5.4 ± 1.1	–
Ta	3.2 ± 0.3	3.2 ± 0.3	3.2 ± 0.2	–
Tb	0.82 ± 0.06	0.82 ± 0.11	0.82 ± 0.09	–
Th	21.4 ± 1.1	21.5 ± 2.2	21.4 ± 0.4	–
Tm	0.53 ± 0.06	0.48 ± 0.09	0.46 ± 0.08	–
U	7.8 ± 0.7	7.8 ± 0.9	7.9 ± 1.6	–
W	37 ± 2	39.9 ± 1.3	37.9 ± 0.6	47 ± 9
V	47 ± 4	–	–	–
Yb	3.7 ± 0.4	3.7 ± 0.2	3.8 ± 0.2	–
Zn	498 ± 18	497 ± 14	482 ± 18	–
Zr	234 ± 16	236 ± 19	231 ± 24	

Validation

To verify the neutron flux parameters determined for selected facilities and assess the applicability of the k_0-INAA method at our research reactor, we analyzed a geological certified reference material (CRM GSD12) and a biological standard reference material (SRM NIST 1573a, Tomato Leaves). The measured results, along with the certified values, are presented in Table 4 respectively. The uncertainties for certified values are reported at a 95% confidence level (k = 2), as specified by the reference material manufacturers. It is important to note that SRM NIST 1573a includes both certified and non-certified elements. For non-certified elements such as Ba, Br, Ce, Cs, Cl, La, Mg, Sc, Sr, and Th, uncertainties were estimated using the modified Horwitz function [27, 34, 35]:

$$\sigma = \begin{cases} 0.22c & if \quad c < 1.2x10^{-7}; \\ 0.02c^{0.8495} & if \quad 1.2x10^{-7} \le c \le 0.138; \\ 0.01c^{0.5} & if \quad c > 0.138; \end{cases} \tag{2}$$

where c is the dimensionless mass ratio (e.g., 1mg $kg^{-1} = 10^{-6}$).

Quality Assessment

The accuracy of the results was assessed using both the ratio of measured to certified values and the Zeta-score (ζ-score) test, which provides a statistical comparison between experimental and certified values, taking into account their respective uncertainties. In accordance with *ISO 13528* [36], the ζ-score is calculated as follows:

$$\zeta = \frac{x_m - x_a}{\sqrt{u_m^2 + u_a^2}} \tag{3}$$

where x_m and x_a are the measured and assigned values of the elemental concentration, respectively; and u_m and u_a are the corresponding combined standard and assigned uncertainty, respectively. A ζ-score within the range of ± 2 indicates acceptable agreement.

Geological Matrix (CRM GSD12)

The results for the geological matrix CRM GSD12, analyzed across three distinct irradiation facilities IB1#A2, IB1#B3, and PTS#R2 are comprehensively presented in * MERGEFORMAT Table 3. A total of 36 elements were successfully quantified, showcasing the effectiveness of the applied neutron activation analysis methods. Across all facilities, the experimental-to-certified value ratios for most elements were observed to be below unity, which indicates a slight systematic underestimation in comparison to certified values. Despite this trend, slight deviations from certified values were identified for specific elements: Br, Cr, and Lu in samples irradiated in the IB1#A2 and IB1#B3 facilities.

The deviation observed in Br concentration determined using the k_0-NAA technique is primarily attributed to the volatility of bromine. during irradiation, such as losses

Table 4 Analytical results of the SRM NIST 1573a (unit: mg/kg)

Element	Certified ± Unc (k = 2)	This work ± Unc (k = 2) at		
		IBI-A2	IBI-B3	PTS-R2
Al	598.4 ± 7.1	–	–	630 ± 85
As	0.1126 ± 0.0024	0.112 ± 0.004	0.118 ± 0.005	–
Ba*	63	64 ± 5	63.89 ± 3.57	–
Br*	1300	1149 ± 13	1310 ± 200	1311 ± 119
Ca	50,450 ± 550	–	–	49,390 ± 3443
Ce*	2	1.79 ± 0.18	2.10 ± 0.05	–
Co	0.5773 ± 0.0071	0.569 ± 0.06	0.575 ± 0.002	–
Cs*	0.053	0.051 ± 0.008	0.0569 ± 0.004	–
Cl*	6600	–	–	6594 ± 457
Cr	1.988 ± 0.034	2.01 ± 0.02	2 ± 0.09	–
Fe	367.5 ± 4.3	365 ± 17	368.6 ± 5.9	–
K	26,760 ± 480	26,700 ± 2500	27,100 ± 264	26,030 ± 5882
La*	2.3	2.5 ± 0.2	2.21 ± 0.01	–
Mg*	12,000	–	–	12,017 ± 831
Mn	246.3 ± 7.1	–	–	247 ± 21
Na	136.1 ± 3.7	136 ± 11	133.6 ± 7.0	137 ± 18
Rb	14.83 ± 0.31	14.61 ± 0.83	14.68 ± 2.10	–
Sb	0.0619 ± 0.0032	0.063 ± 0.01	0.0654 ± 0.002	–
Sc*	0.1	0.09 ± 0.01	0.105 ± 0.001	–
Th*	0.12	0.11 ± 0.004	0.114 ± 0.004	–
Zn	30.94 ± 0.5	29.95 ± 0.90	31.08 ± 0.94	–

NB: (*) indicate the informative value in SRM-NIST1573a

owing to volatilization and migration of bromine from the sample matrix through the walls of pure aluminum bags. This loss leads to an underestimation of its true concentration.

In the case of Cr, the overestimation is mainly due to spectral interferences, particularly around the 320 keV region. This region may suffer from peak overlap or poor resolution, causing an inflated estimation of Cr activity.

As for Lu, the deviation is likely related to the neutron absorption behavior of its isotope. Unlike most isotopes that follow the 1/v law, lutetium does not strictly adhere to this trend and is highly sensitive to temperature variations within the irradiation facility. Such sensitivity can introduce inaccuracies in the calculated concentration if not properly accounted for.

For PTS#R2, which focuses on short-lived nuclides due to its rapid analytical capabilities, minor deviations were noted specifically for In. These results underscore the challenges associated with accurately quantifying certain elements and the inherent variability in measurement conditions across irradiation facilities.

The ζ-score evaluation, a robust metric for assessing the agreement between measured and certified values, further validated the accuracy of the analytical processes employed. For samples irradiated in IB1#A2 and IB1#B3, the majority of ζ-scores were within the ± 1 range, indicative of excellent agreement with certified values. Only two elements, Cr and Lu, exhibited ζ-scores outside the ± 2 range. While this remains within an acceptable margin, it indicates the need for careful calibration or methodological adjustment when analyzing these elements. Notably, all ζ-scores for elements analyzed in PTS#R2 were below ± 1 range, demonstrating an exceptional level of consistency and reliability for short-lived elements in this irradiation setup.

Figure 3 provides a detailed visual representation of the experimental-to-certified value ratios and corresponding ζ-scores for CRM GSD12 across the three facilities. This graphical analysis highlights the comparative performance of each facility and allows for a nuanced interpretation of the dataset.

The observed consistency across irradiation setups reinforces the robustness of the experimental procedures and validates the suitability of the facilities for high-precision elemental analysis of geological matrices. These results also contribute to valuable insights for refining analytical methodologies and improving accuracy for challenging elements such as Br, Cr and Lu.

Biological Matrix (SRM NIST 1573a)

The analytical results for the biological matrix SRM NIST 1573a, determined across three irradiation facilities (IB1#A2, IB1#B3, and PTS#R2), are comprehensively detailed in Table 4. A total of 16 elements were quantified for samples irradiated in IB1#A2, IB1#B3. For both facilities, the experimental-to-certified value ratios were consistently below unity, suggesting a slight underestimation in the measured concentrations relative to certified values. This

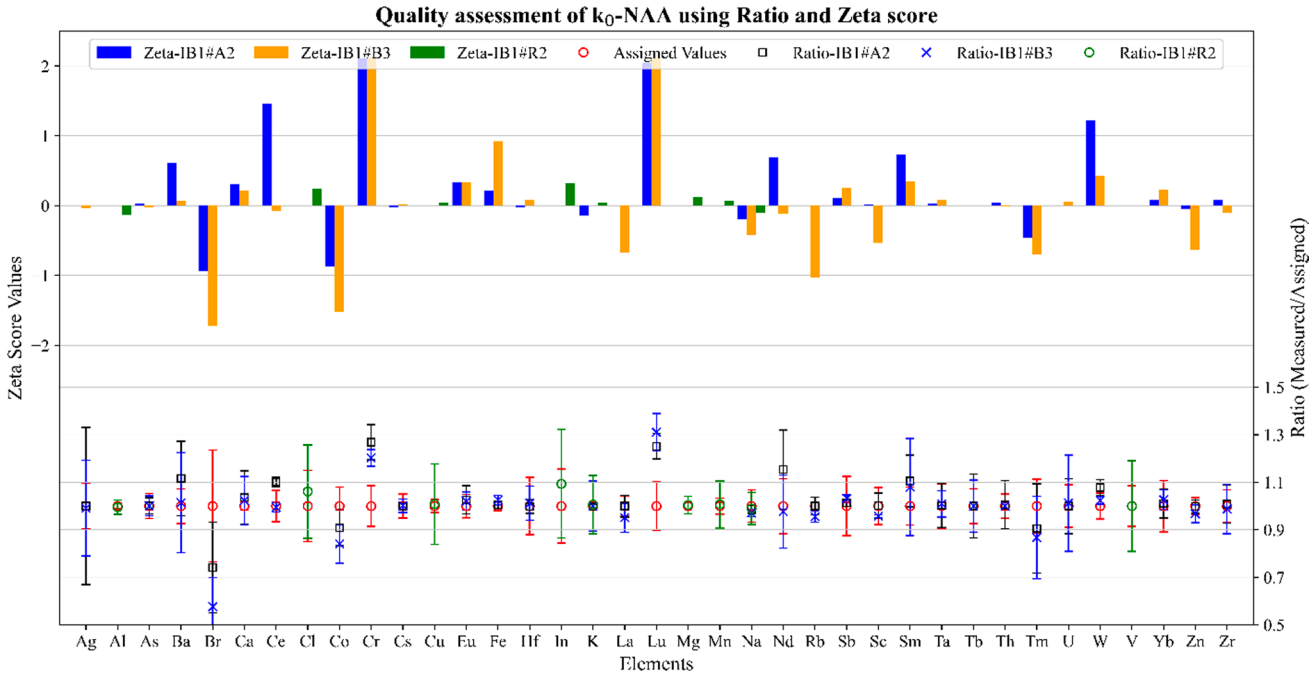

Fig. 3 The Ratio and ζ-score for the measured concentrations in CRM GSD12 reference materials irradiated in three selected facilities

trend indicates the need to refine the calibration or correction factors applied during the quantification process. Additionally, eight (08) short-lived elements were analyzed after irradiation in PTS#R2, a facility optimized for such analyses. The results for these elements mirrored the trend observed in the other two facilities, with ratios also consistently below unity, reaffirming the reliability of the analytical protocols employed.

The ζ-score evaluation, a statistical measure that assesses the agreement between experimental and certified values, further reinforced the high level of accuracy achieved. For IB1#A2, the majority of ζ-scores were well within the ± 1 range, indicating an excellent agreement with certified values. Notable exceptions included Ce (1.16), Th (1.16), and Br (1.9), which slightly exceeded the ± 1 threshold but remained within the acceptable range for analytical variability. Similarly, for IB1#B3, most elements demonstrated ζ-scores below ± 1, with a few exceptions, including Ce, La, Sc, and Th, suggesting room for improvement in the measurement precision for these elements in this particular facility.

In contrast, the PTS#R2 facility demonstrated exceptional performance in the analysis of short-lived elements, as all ζ-scores fell below ± 0.5 range. This superior level of agreement highlights the precision and reliability of the rapid neutron activation analysis techniques employed at this facility, particularly for elements with shorter half-lives.

This graphical analysis in Fig. 4 illustrates the strong overall agreement between measured and certified values, with minor deviations for a few elements. The consistently low ζ-scores across all facilities confirm the robustness of the analytical methods and emphasize the reliability of the facilities for the precise quantification of elements in biological matrices. These results contribute valuable insights for optimizing methodologies, particularly for challenging elements such as Ce, Th, and Br, ensuring continuous improvement in analytical accuracy.

The validation results for both the geological matrix CRM GSD12 and the biological matrix SRM NIST 1573a demonstrate a high level of consistency and agreement with certified values across all three irradiation facilities. Minor deviations observed for certain elements highlight areas for methodological refinement, while the consistently low ζ-scores confirm the robustness and reliability of the applied analytical techniques, reinforcing the suitability of these facilities for precise multi-element quantification.

Conclusion

The project of implementing the k_0-NAA method at the NUR research reactor marks a significant milestone in the advancement of nuclear analytical techniques in Algeria. Building on the successful implementation of this method at the Es-Salam Research Reactor in 2004, the NUR reactor now provides a new platform for high-precision elemental analysis using Neutron Activation Analysis (NAA).

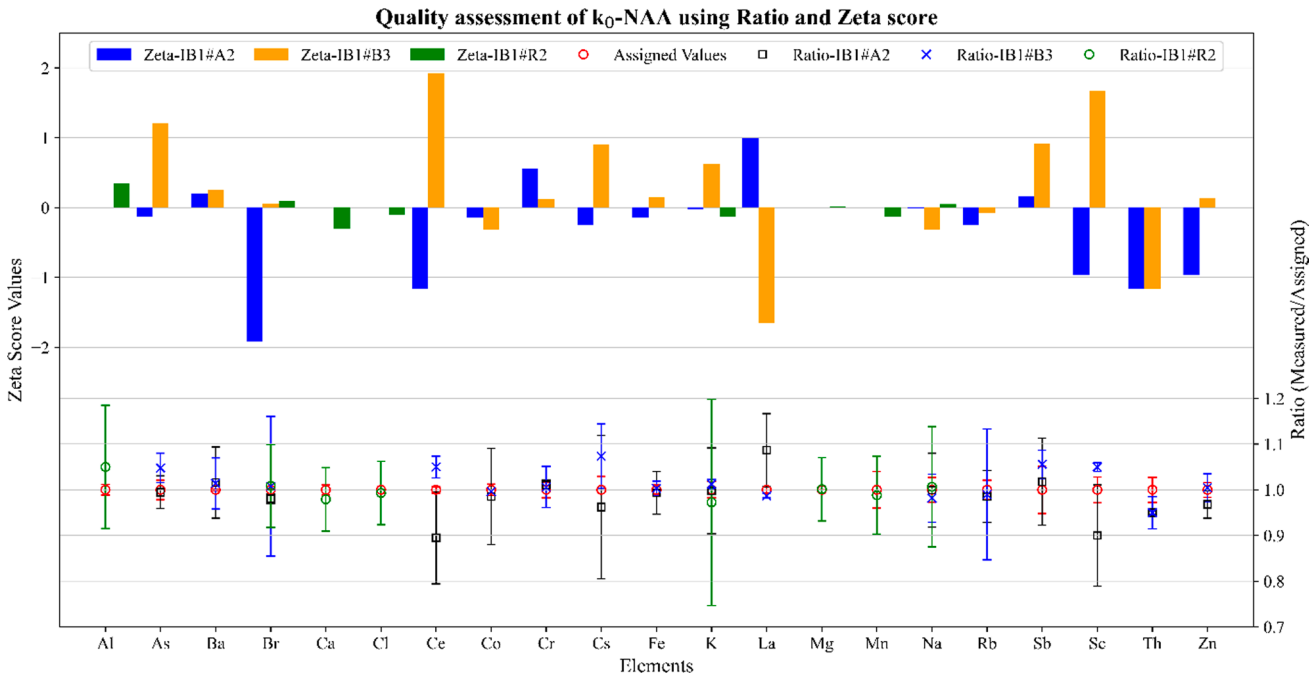

Fig. 4 The Ratio and ζ-score for the measured concentrations in SRM NIST 1573a reference materials irradiated in three selected facilities

This project aims to further develop and optimize the k_0-NAA methodology, ensuring that the NUR reactor can effectively support the reliable and accurate measurement of trace and major elements in various sample matrices, including geological and biological materials. The implementation involved determining key neutron flux parameters, such as the thermal and fast neutron fluxes and the α and f values, critical for the accurate application of the k_0-NAA technique.

Through rigorous testing and validation with certified reference materials (CRM GSD12 and SRM NIST 1573a), the study demonstrated the effectiveness and reliability of the k_0-NAA method at the NUR reactor. The use of this method in Algeria's nuclear research infrastructure enhances the country's capability to perform advanced elemental analyses with a high degree of precision, establishing the NUR research reactor as a key facility for nuclear research and analytical applications in the region.

This achievement paves the way for the exploitation of the k_0-INAA method in practical future applications, particularly for the analysis of complex matrices, where accurate multi-elemental quantification is essential for environmental, health, and industrial studies.

Acknowledgements The authors extend their heartfelt gratitude to Dr. M.N. Boucherit, Director General of the Nuclear Research Center of Draria, for his steadfast support and encouragement throughout this project. We express our deep appreciation to A. Ameur, M. Azzoune, M. Mokrani, R. Zamoun, D. Lababsa, A. Aknoun and O. Omrani for their invaluable assistance and motivation. We also wish to acknowledge our colleagues from the Operations Service, the Radiation Protection Officers at the NUR reactor facility, and the Neutron Activation Analysis (NAA) Laboratory team. Their unwavering support and valuable contributions have significantly enriched this work. Finally, we extend our sincere thanks to our colleagues from the Energy and Materials Laboratory at the University of Tamanghasset for their collaboration and support.

Declarations

Conflict of interest There is no conflict of interest of any kind whatsoever.

References

1. Meftah B, Zidi T, Bousbia-Salah A (2006) Neutron flux optimization in irradiation channels at NUR research reactor. Ann Nucl Energy 33(14–15):1164–1175. https://doi.org/10.1016/j.anucene.2006.08.003
2. Mazidi S, Meftah B, Belgaid M, Letaim F, Halilou A (2015) ITHNA.SYS: An integrated thermal hydraulic and neutronic analyzer SYStem for NUR research reactor. Nucl Eng Des 289:175–185. https://doi.org/10.1016/j.nucengdes.2015.04.025
3. Mazrou H, Lababsa D, Mokhtari O (2023) Assessment of the safety impact caused by the variations of the critical position of control rods and by the presence of an in-core flux trap on the power peaking factors in an MTR-type research reactor. Nucl Eng Des 414:112553. https://doi.org/10.1016/j.nucengdes.2023.112553
4. Lababsa D, Mazrou H, Belgaid M (2024) Performance evaluation and validation of OpenMC code for criticality analysis of an MTR-type research reactor. Ann Nucl Energy 206:110617. https://doi.org/10.1016/j.anucene.2024.110617
5. Lababsa D et al (2025) Software-based automation of burnup calculations for the NUR research reactor using SCALE/TRITON T6-DEPL sequence. Ann Nucl Energy. https://doi.org/10.1016/j.anucene.2024.111007
6. A. Mansouri, M. Mouzai, and L. Hamidatou-Alghem, determination De la concentration du zinc dans les cheveux des femmes atteintes du cancer du sein par l'analyse par Activation Neutronique Instrumentale (INAA), 2015. Available: https://www.researchgate.net/publication/283928547
7. Bouhila Z et al (2015) Investigation of aerosol trace element concentrations nearby Algiers for environmental monitoring using instrumental neutron activation analysis. Atmos Res 166:49–59. https://doi.org/10.1016/j.atmosres.2015.06.013
8. Azli T et al (2021) Application of instumetal neutron activation analysis method for determination of some trace elements in lichens around three sites in Algiers. Radiochim Acta 109(9):719–725. https://doi.org/10.1515/ract-2021-1050
9. Mansouri A et al (2021) Instrumental neutron activation analysis (INAA) of zinc concentrations in scalp hair and fingernails samples of Algerian females with breast cancer. Radiochim Acta 109(12):915–923. https://doi.org/10.1515/ract-2021-1069
10. F. De Corte and J. Hoste, Single-comparator methods in reactor neutron activation analysis, 1975.
11. C. O. Mustra, M. C. Freitas, and S. M. Almeida, Neutron flux and associated k 0 parameters in the RPI after the last configuration change, 2003.
12. Alghem L, Ramdhane M, Khaled S, Akhal T (2006) The development and application of k0-standardization method of neutron activation analysis at Es-Salam research reactor. Nucl Instrum Methods Phys Res A 556(1):386–390. https://doi.org/10.1016/j.nima.2005.10.017
13. Siong WB, Dung HM, Wood AK, Salim NAA, Elias MS (2006) Testing the applicability of the k0-NAA method at the MINT's TRIGA MARK II reactor. Nucl Instrum Methods Phys Res A 564(2):716–720. https://doi.org/10.1016/j.nima.2006.04.012
14. Wasim M, Arif M, Zaidi JH, Anwar Y (2009) Development and implementation of K0-INAA standardization at 10 MW Pakistan research reactor-1. Radiochim Acta 97(11):651–655. https://doi.org/10.1524/ract.2009.1657
15. Mariano DB, Figueiredo AMG, Semmler R (2014) Implementation of the k 0-standardization method for analysis of geological samples at the Neutron Activation Analysis Laboratory, São Paulo, Brazil. J Radioanal Nucl Chem 299(1):725–731. https://doi.org/10.1007/s10967-013-2696-3
16. Esen AN, Haciyakupoglu S (2016) Implementation of k0-INAA standardisation at ITU TRIGA Mark II research reactor, Turkey based on k0-IAEA software. Radiat Phys Chem 119:282–286. https://doi.org/10.1016/j.radphyschem.2015.11.013
17. Moon JH, Kim SH, Senjlawi Y (2019) Measurement of neutron spectrum parameters for NAA irradiation holes in the Jordan research and training reactor. J Radioanal Nucl Chem 322(3):1525–1528. https://doi.org/10.1007/s10967-019-06821-1
18. De Corte F (2018) The k 0-standardization of NAA: germs, launch, breakthrough—on stage and in the wings. J Radioanal Nucl Chem. https://doi.org/10.1007/s10967-018-6254-x
19. L. Alghem Hamidatou and M. Ramdhane, Characterization of neutron spectrum at Es-Salam Research Reactor using Høgdahl convention and Westcott formalism for the k0-based neutron activation analysis, *J Radioanal Nucl Chem*, vol. 278, no. 3, pp. 627–630, 2008, https://doi.org/10.1007/s10967-008-1205-6.

20. Hamidatou L, Benkharfia H (2011) Experimental and MCNP calculations of neutron flux parameters in irradiation channel at Es-Salam reactor. J Radioanal Nucl Chem 287(3):971–975. https://doi.org/10.1007/s10967-010-0922-9
21. Hamidatou L, Slamene H, Akhal T, Boulegane A (2014) Trace and essential elements determination in baby formulas milk by INAA and k0-INAA techniques. J Radioanal Nucl Chem 301(3):659–666. https://doi.org/10.1007/s10967-014-3213-z
22. Hamidatou L, Slamene H, Mohamed LS (2015) Major, minor and trace elements in four kinds of cement powder using INAA and k 0-standardization methods. J Radioanal Nucl Chem 304(2):717–725. https://doi.org/10.1007/s10967-014-3839-x
23. Samanta SK, Sengupta A, Acharya R, Pujari PK (2021) Standardization and validation of k0-based neutron activation analysis using Apsara-U reactor and its application to pure iron metal and coal sample for trace element determination. Nucl Instrum Methods Phys Res A 1018:165856. https://doi.org/10.1016/j.nima.2021.165856
24. Hamidatou L, Arbaoui F, Chahra R, Slamene H, Djebli K, Boucherit MN (2024) Determination of rare earth elements in Algerian bentonites using k_0 -NAA method. Radiochim Acta 112(1):45–52. https://doi.org/10.1515/ract-2023-0210
25. Frans De Corte, The k0-standardization Method. A Move to the Optimization of Neutron Activation Analysis, Ghent University, 1987.
26. H. M. Dung and F. Sasajima, Characterization of detectors and irradiation facilities determination of and f for k 0-NAA in irradiation sites with high thermalized neutrons, 2003.
27. Moon J-H, Kim S-H, Chung Y-S, Kim Y-J (2007) Application of the k 0-NAA method at the HANARO research reactor. J Radioanal Nucl Chem. https://doi.org/10.1007/s10967-007-0206-1
28. A. Simonits, F. De Corte, and § J Hoste, Zirconium as a multi-isotopic flux ratio monitor and a single comparator in reactor-neutron activation analysis, 1976.
29. HyperLab 2023 Gamma Spectroscopy Software Manuals HyperLabs Software, 1998.
30. F. De Corte *et al.*, Installation and calibration of Kayzero-assisted NAA in three Central European countries via a Copernicus project, 2001.
31. Kayzero for Windows. [Online]. Available: www.kayzero.com
32. Azli T, Chaoui ZEA (2015) Performance revaluation of a N-type coaxial HPGe detector with front edges crystal using MCNPX. Appl Radiat Isot 97:106–112. https://doi.org/10.1016/j.apradiso.2014.12.027
33. van Sluijs R, Blaauw M (2023) Defining 'k f-factors' for threshold reactions. J Radioanal Nucl Chem 332(6):1835–1840. https://doi.org/10.1007/s10967-023-08871-y
34. Thompson M (2000) Recent trends in inter-laboratory precision at ppb and sub-ppb concentrations in relation to fitness for purpose criteria in proficiency testing. Analyst 125(3):385–386. https://doi.org/10.1039/b000282h
35. Chung YS, Dung HM, Moon JH, Park KW, Kim HR (2006) Implementation of the k0-NAA method in the NAA#3 irradiation hole of the HANARO research reactor. Nucl Instrum Methods Phys Res A 564(2):702–706. https://doi.org/10.1016/j.nima.2006.04.014
36. ISO 13528:2015(E) II Copyright Protected Document, 2015. [Online]. Available: www.iso.org